

Hierarchy Structure in Injection Molded Polypropylene/Ethylene–Octane Copolymer Blends

Jiang Li, Xiaoqing Zhang, Cheng Qu, Qin Zhang, RongNi Du, Qiang Fu

Department of Polymer Science and Materials, State Key Laboratory of Polymer Materials Engineering, Sichuan University, ChengDu 610065, People's Republic of China

Received 1 May 2006; accepted 14 November 2006

DOI 10.1002/app.26225

Published online 26 April 2007 in Wiley InterScience (www.interscience.wiley.com).

ABSTRACT: In this article, the phase morphology and mechanical properties of polypropylene (PP)/ethylene–octane copolymer (POE) blends with fixed ratio (60/40) obtained via different processing conditions, including barrel temperature, injection speed, and mold temperature, have been investigated. SEM was carried out for detailed characterization of phase morphology from the skin to the core, layer by layer. It was interesting that for all the processing conditions no dispersed POE elastomer was observed in the skin layer but elongated POE particles with large size were observed in the subskin layer. From the transition zone to the core layer, an increased phase separation was observed, which could lead to a formation of cocontinuous morphology, depending on the processing condition used. Higher barrel temperature,

lower mold temperature, and higher injection speed could result in a smaller size of POE phase. The tensile strength and impact strength were found not sensitive to barrel temperature and mold temperature but to the low injection speed, both tensile strength and impact strength had a higher value for specimen obtained via low injection speed. The formation of the skin-core morphology and the effect of processing conditions on the phase morphology were discussed based on crystallization kinetics of PP matrix, rheology, and shear induced phase mixing. © 2007 Wiley Periodicals, Inc. *J Appl Polym Sci* 105: 2252–2259, 2007

Key words: skin-core structure; phase morphology; PP/POE blend; injection molding

INTRODUCTION

Injection molding is a widely extended process characterized by high production rate and tight geometrical tolerances. In this process, a hot polymer melt is forced under pressure to flow between cold mold walls, and the high viscous melt has a complex behavior such as shear thinning and viscoelastic nature.¹ A large number of processing conditions are available in the injection molding process, including barrel and mold temperatures, injection speed, hold pressure, back pressure, etc.,² resulting in fruitful crystal and phase morphologies in the molded samples. Li et al.³ pointed out that all parameters, including thermal and mechanical history, thermal transitions, or the condition of the thermal characterization, need to be designed carefully for an unambiguous interpretation and discussion of the results. Due to the shear stress and thermal gradients, usually,

injection molded parts contain a hierarchy of macromolecular arrangements and a skin-core structure. In the two external skin layer, the highly oriented crystalline can be found and a large number of spherulite exist in the core layer. Between these two layers a transition zone are commonly found presenting deformed spherulite structures typically associated to the crystallization under high shear and temperature gradients.^{4–9}

The morphology of heterogeneous polymeric systems, such as immiscible polymer blends or fiber reinforced polymers, becomes very complicated because of the complex conditions in the processing. Karger-Kocsis¹⁰ is one of the earliest researchers to study the morphology of injection molded parts of polymer blends. It was observed that the skin-core morphology contained a pure matrix in the skin layer and deformed rubber particles along the flow direction in the subskin layer. Fellahi et al.¹¹ studied injection molded HDPE/Polyamide-6 blends, and a dispersed phase with very tiny size in skin layer was reported. It was explained that the skin layer was formed by the fountain flow at the flow front and by shear flow on the frozen layer when it comes to subskin layer. Younggon et al.¹² observed clearly the elongated particles in the skin layer in poly(phenylene oxide)/polyamide-6 blends.

Study of the property and morphology of polyolefin blends has always received great interests, not

Correspondence to: Q. Fu (qiangfu@scu.edu.cn).

Contract grant sponsor: National Natural Science Foundation of China; contract grant numbers: 20404008, 50533050, 20490220.

Contract grant sponsor: Major State Basic Research Projects of China; contract grant number: 2003CB615600.

Contract grant sponsor: Ministry of Education of China; contract grant number: 104154.

Journal of Applied Polymer Science, Vol. 105, 2252–2259 (2007)
© 2007 Wiley Periodicals, Inc.

only because of their wide application in industry, but more importantly because of their rich and fascinating morphology depending on molecular structure, thermal history, and external stress field.^{13,14} The recent finding that shear could induce phase dissolution^{15,16} at a higher shear rate provides a possibility that modulating the phase morphology, using high shear rate via injection molding.

Isotactic polypropylene (iPP) is a semicrystalline polymer, which has been used in a wide variety of industrial applications, mainly because of its ease of processing, low density, good stiffness, and relatively low cost. The application of polypropylene (PP), however, has been limited by its tendency to brittleness at temperature below its glass transition temperatures. To overcome this limitation, numerous studies have been carried out to improve the toughness with balanced stiffness and modulus. In recent years, ethylene-octane copolymer (POE) has attracted increasingly interests in the modification of iPP, because of its good toughening effect compared with other elastomers.¹⁷ iPP and POE could be phase miscible or immiscible depending on the composition and the content of octane branching.¹⁸ The copolymer is immiscible with iPP in the molten state if the α -olefin content is less than 50 mol % and miscible with amorphous phase of iPP if it is more than 50 mol %.¹⁹ In the present work, to better understand the morphology development and structure change of PP/POE blends during injection processing, detailed phase morphology of PP/POE blends with fixed ratio (60/40) under different injection molding conditions were investigated by using scanning electron microscopy (SEM). We are seeking to establish a fundamental understanding of structure-property-processing relationships through the control of phase separation, molecular orientation and crystal morphology of iPP/POE blends, as part of long-term project aimed at super polyolefin blends.

EXPERIMENTS

Materials

The iPP and POE used in experiment are commercial products. iPP (T30S, melt flow index is 2.3 g/10 min) was purchased from the Du Shanzi Petroleum Chemical, China; POE (8150, octane content is 25%, melt flow index is 0.5 g/10 min) was from Du Pont, USA.

Sample preparation

The blend containing 40 wt % of POE was extruded and granulated on a twin-screw extruder (TSSJ-25 corotating twin-screw extruder). The temperatures were set at 160, 190, 200, 200, and 195°C from the hop-

per to the die and the screw speed was about 120 r/min. After making droplets, the blends were fed into an injection-molding machine (PS40E5ASE, Japan) to prepare the specimens. And the dumbbell-shaped bars were obtained for structural characterizing and mechanical properties testing. The processing variables that can be changed in our injection-molding machine during the experiment are: barrel temperature, injection speed, and mold temperature. A design of experiment method¹ was used to perform a sequence of runs under different sets of processing conditions. Samples No. 1–3, have the same injection speed and mold temperature but different barrel temperatures; samples No. 4–6 have the same barrel temperature and mold temperature but different injection speeds; samples No. 7–9 have the same barrel temperature and injection speed but different mold temperatures. The high and low values of each of the three processing parameters are shown in Table I. And the thickness of the bars is 4 mm.

SEM experiments

The blend samples prepared from different injection-molding conditions were fractured at the same depth from the outmost surface of bars for comparison. After that, the phase morphologies of all the blends were studied by preferential etching of the dispersed phase in dimethylbenzene at 32°C for 1 h. Then the morphologies in each layer from skin to core were obtained in an SEM instrument, JSM-5900LV, with an accelerating voltage of 20 kV.

Mechanical properties measurements

Tensile tests were performed by a Shimadzu AG-10TA Universal Testing Machine at a crosshead speed of 50 mm/min at room temperature. For impact strength tests, the notched specimens were tested with an I200XJU-2.75 impact tester at room temperature, and the notches with 45° were made by machine, according to ISO 179. The values of all the mechanical parameters are calculated as averages

TABLE I
Conditions for Injection Molding

Run no.	Barrel temperature (°C)	Injection speed (%)	Mold temperature (°C)
1	210	14	23
2	230	14	23
3	250	14	23
4	210	5	23
5	210	20	23
6	210	25	23
7	210	14	50
8	210	14	80

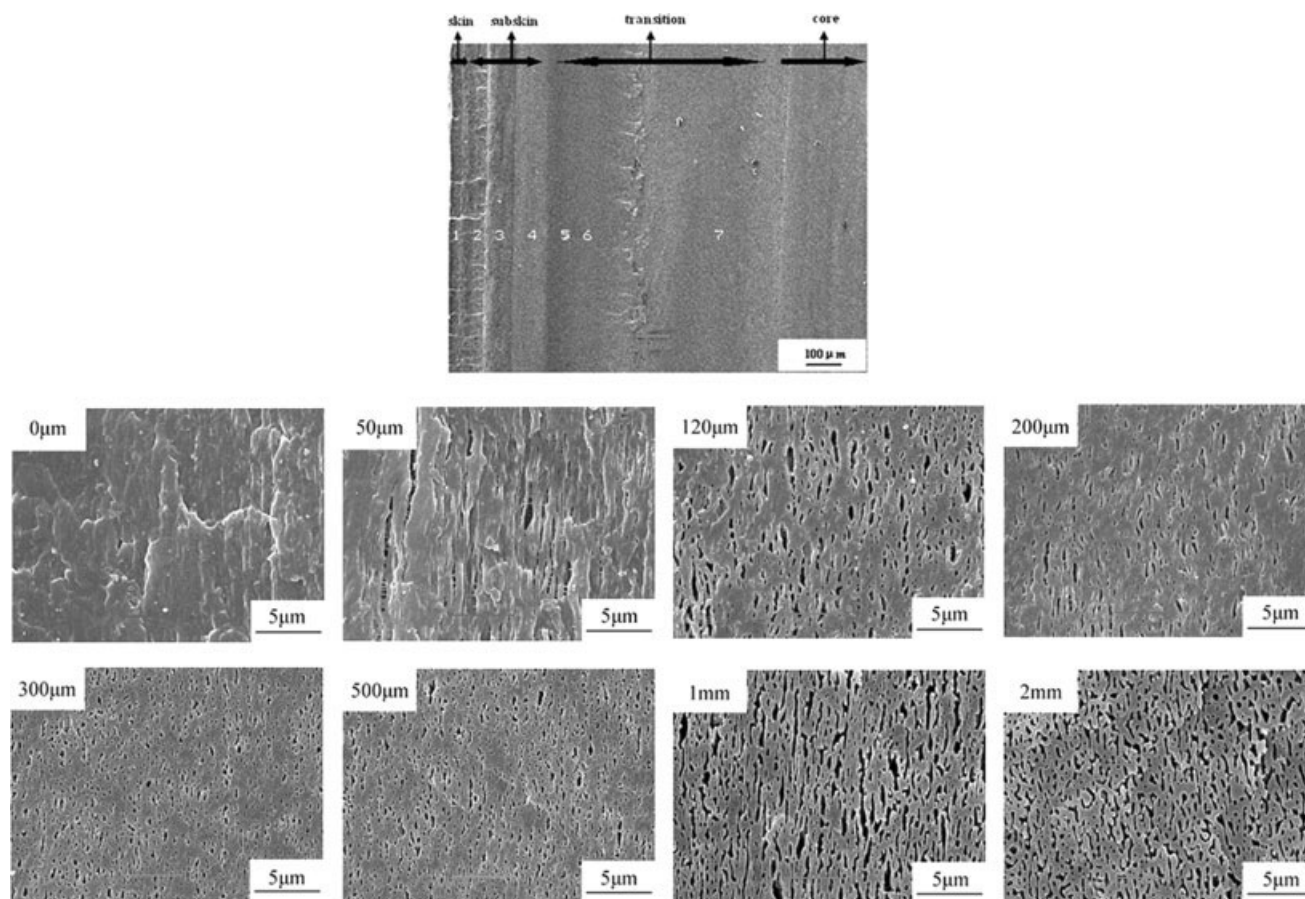


Figure 1 SEM photos of the sample No. 1 from skin to core. The upper one is SEM micrograph in low magnification, the numbers on the top left corner show the distance to the surface of the bar.

over 6–9 specimens for each injection molding condition.

RESULTS

Skin-core morphology

The characterization of microstructure and phase morphology in injection-molded bars is complex because of the existence of a shear gradient and a temperature gradient from the skin to the core, so skin-core morphology with different orientation, phase separation and lamella size along the thickness direction of molded bars is expected. For example, Figure 1 shows the multilayer structure of phase morphology of sample No. 1. Various morphologies in different layers in a specimen from skin to core can be obviously seen in the upper one of Figure 1 because of the shear gradient and temperature gradient during the solidification. The bottom eight micrographs represent the phase morphologies in much larger magnification in the different positions of the specimen, and the markers on the top left corner show the distance from surface to the layer. The skin layer is about 40 μm and very little POE elastomer can be

found in this layer. The phase morphology evolution from the subskin layer to the core can be clearly seen from 50 μm to 2 mm (the thickness of the specimen is 4 mm). From 50 μm to 200 μm , oriented elastomer particles can be easily found in this zone and the size of the dispersed phase becomes smaller. Then the size of elastomer particles becomes bigger and the phase morphology transforms from droplet/matrix to cocontinuous as further going to the center.

Effect of barrel temperature

The thermal field during the processing is one of the most important factors that may affect the compatibility and the viscosity ratio of the blend system. To find out this effect on the phase morphology in the injection-molded samples, a series of SEM were carried out on the samples No. 1–3, and the results are shown in Figure 2. In these photos, the upper row represents the samples injection-molded at barrel temperature 210°C from skin to core, and the bottom one represents the specimens injection-molded at barrel temperature 250°C. Furthermore, the SEM photos in the same column come from the same part of the

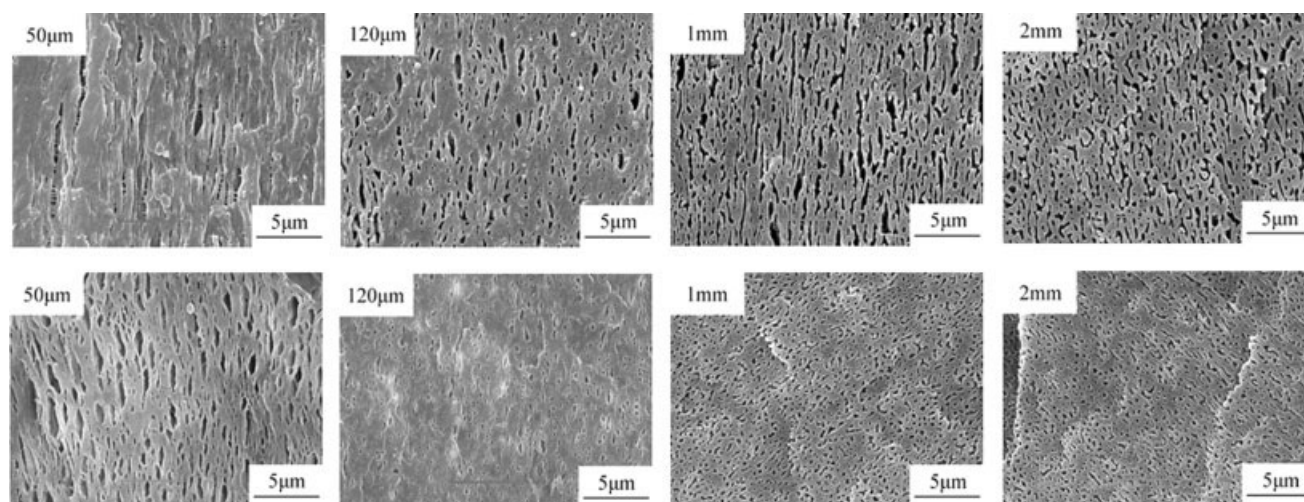


Figure 2 SEM micrographs of sample Nos. 1 and 3. The upper row shows hierarchy structure of sample No. 1 across the thickness from skin to core, the bottom row shows hierarchy structure of sample No. 3 across the thickness from skin to core. The numbers on the top left corner in each picture represent the distance to the surface of the samples.

specimen for comparison. One observes elongated elastomers at the subskin layer for both conditions, but the aspect ratio is smaller for the samples obtained via higher barrel temperature. The size of dispersed phase of samples molded at barrel temperature 250°C is much smaller, even in the core layer, and the phase morphology is still as droplet/matrix and the dispersed phase size is about 0.2 μm. Whereas the phase morphology of samples molded at barrel temperature 210°C, has a much bigger particle size, and develops into the cocontinuous in the core with a size of 1 μm.

Effect of injection speed

The role of the injection speed on the hierarchy structure in the sample is also investigated, and the SEM pictures are shown in Figure 3. The upper row represents the sample via 5% injection speed, whereas the bottom one represents that via 25% injection speed. Generally, higher injection speed induces higher shear stress on the melt in the mold, and higher orientation or more elongated dispersed phase. It is out of expectation that much larger and more elongated particles were found in subskin layer of the sample obtained via 5% injection speed (sample No. 4), compared with those of the sample No. 6, which was obtained via 25% injection speed. In the core layer, the orientation of POE phase becomes weak, regardless of the different injection speed.

Effect of mold temperature

Usually, higher mold temperature can provide more time for the phase separation for immiscible polymer blends. The phase morphologies of samples obtained

with different mold temperatures are shown in Figure 4. Compared with the one obtained at cold mold temperature, the high-mold-temperature sample possesses larger dispersed phase and less obvious hierarchy structure.

Mechanical properties

The mechanical properties, including the yield strength and impact strength, are correlative to the phase morphology. The tensile stress and the impact strength were tested to investigate the relationship among the processing conditions, morphology structures and the properties. Figure 5 shows the stress–strain curves of those samples obtained at different processing conditions, and the tensile stress and impact strength are listed in Table II. Very interestingly, it can be found that the tensile strength and impact strength were found not sensitive to barrel temperature and mold temperature, but as to the specimens obtained via low injection speed, both tensile strength and impact strength had the highest values. The tensile strength should be mainly related to the orientation of PP matrix and this needs 2d-WAXD or 2d-SAXS to calculate the molecular or lamellar orientation of PP via different processing conditions. For the impact strength, however, not only the molecular orientation, but also the phase and crystal morphology will play very important role in determining the toughness.

DISCUSSION

Hierarchy structure of the dispersed phase

Due to the existence of a shear gradient and a temperature gradient from the skin to the core, not only the

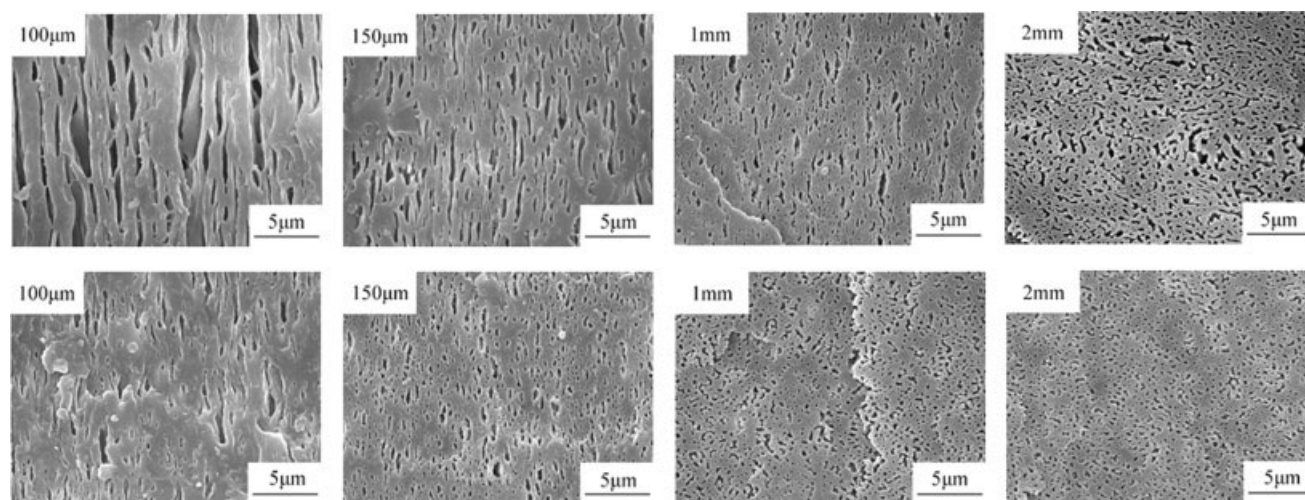


Figure 3 SEM micrographs of sample Nos. 4 and 6. The upper row shows hierarchy structure of sample No. 4 across the thickness from skin to core, the bottom row shows hierarchy structure of sample No. 6 across the thickness from skin to core. The numbers on the top left corner in each picture represent the distance to the surface of the samples.

different size and shape can be observed along the sample thickness, but the existence of the distribution of POE content could also be possible. The fact that little POE were found in the skin layer (Fig. 1; 0 μm) could be resulted from (1) a decreased POE content and (2) shear-induced compatibility that the dispersed POE particles were so small as not to be found by SEM observation. Karger-Kocsis¹⁴ also found there does not exit elastomer in the skin layer in his experiments via injection molding of PP/EPR blends. The shear-induced compatibility is worth to be further investigated. However, from the point of crystallization kinetic consideration, the fast crystallization may make the PP reject the rubbery particles rather than occlude them^{20,21} and thus it induces the content gra-

dient. On the other hand, in the view of rheology, the mold cavity can be considered as the pipeline. When the flow of a dilute suspension of spheres in a non-Newtonian medium is examined, the direction of particle migration appears to depend on the relative influence of elasticity and shear thinning.^{22,23} Under the influence of fluid elasticity, particles move from regions of high shear rate to regions of low shear rate; this happens because a gradient in the first normal stress difference results in a “lift force” perpendicular to the streamline direction. Thus, in tube flow, spheres tend to accumulate along the axis, often associating with each other in the form of a necklace, which can be sketched in Figure 6. The effect of shear thinning is opposite to that of fluid elasticity, and it

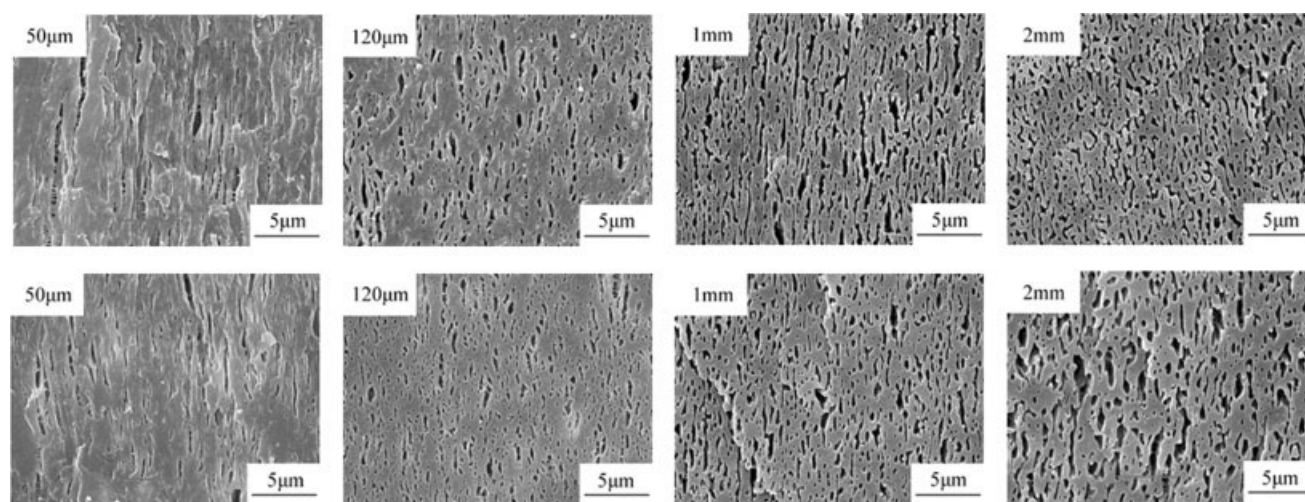


Figure 4 SEM micrographs of sample Nos.1 and 8. The upper row shows hierarchy structure of sample No.1 across the thickness from skin to core, the bottom row shows hierarchy structure of sample No.8 across the thickness from skin to core. The numbers on the top left corner in each picture represent the distance to the surface of the samples.

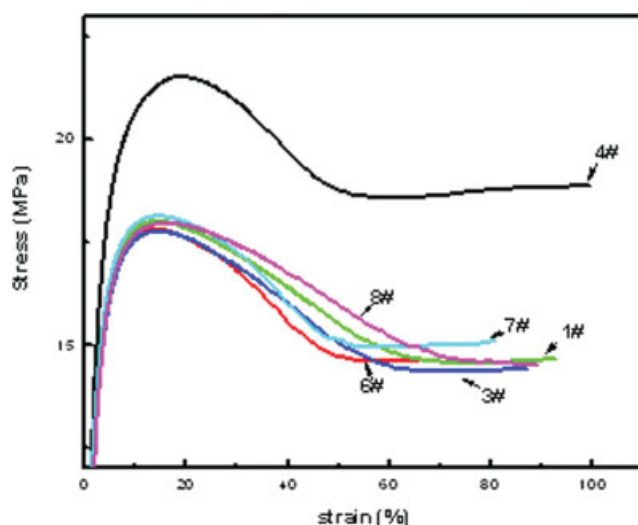


Figure 5 Stress-strain curves of the specimens under different processing conditions. [Color figure can be viewed in the online issue, which is available at www.interscience.wiley.com.]

results in migration in a direction of increasing shear rate. When a viscoelastic fluid is also highly shear thinning, particles move toward the wall in Poiseuille flow but do not actually hit the wall.²³ As going to the center, a large dispersed phase size and the oriented elastomer particles can be easily observed as shown in Figure 1 (50, 120, and 200 μm). Because of the high shear stress during the injection process and the fast quench speed, the POE particles were deformed and held finally. And the aspect ratio became smaller, caused by the decreased shear stress. According to the normal theory, the size should be smaller in the outer parts from the core of the specimens²⁴ because of the shear-induced mixing.⁶ The largest size can be seen in the core (Fig. 1; 2 mm), and this can be understood as the result of higher temperature and decreased shearing stress. The phase morphology is evolved into more stable state under this situation, and finally the cocontinuous morphology is formed. Profiting from the quenching layer by layer in the mold, the evolvement of this hierarchy structure can be clearly demonstrated in our experiment.

TABLE II
Mechanical Properties of Samples Via Different Conditions

Sample no.	Tensile strength (MPa)	Impact strength (kJ/m^2)
1	18.1	57.6
3	17.9	58.3
4	21.5	62.5
6	17.9	56.7
7	18.2	56.2
8	18.0	54.7

Skin thickness

As is seen earlier, the morphology in the skin is quite different from the other parts because of the fast cooling of the melt. Thus studying the skin thickness is of particular interest. Figure 7 shows the SEM photos of the representative samples in low magnification. The overall phase morphologies of these samples can be seen from the photos, and the skin thickness can be estimated directly. In these photos, a, b, c, d, and e represent the samples under normal injection conditions, higher barrel temperature, lower injection speed, higher injection speed and higher mold temperature, respectively. The barrel temperature has no distinct effect on the skin thickness. The samples under lower and higher injection speed have thicker (80–100 μm) and thinner (20–30 μm) skin layer, respectively. For the sample obtained via 80°C mold temperature, the skin thickness is very small (skin thickness: $\sim 10 \mu\text{m}$) and can be ignored. In this case the borderline between skin and subskin layer disappears. It is interesting that larger injection speed induced thinner skin thickness, whereas the skin layer became blurred under higher mold temperature. The high injection speed may induce the high heat because of the friction toward the mold wall, and slow down the crystallization rate of PP around this area. Since the formation of the skin layer was related to the crystallization of PP matrix, its thickness became thinner when the shear stress in the mold was strong. In the same way, when the mold temperature was high, the crystallization rate of PP matrix became slowed down, and a thinner skin was formed.

Phase morphology

The phase separation and shear-induced phase transition in blends are two important factors to control the phase morphology of the specimens. From Figure 2, a smaller size of the dispersed phase for sample obtained via higher barrel temperature suggests a good compatibility of the two phases, and it is reported that the POE (8150) is partially miscible with

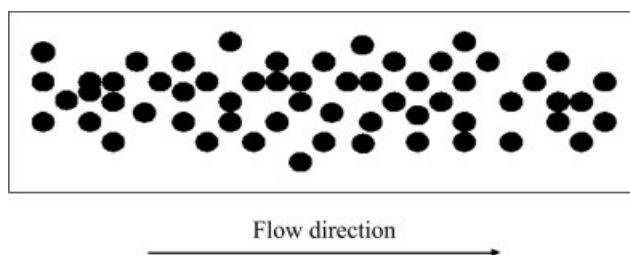


Figure 6 Schematic figure of particles flow in a non-Newtonian medium.

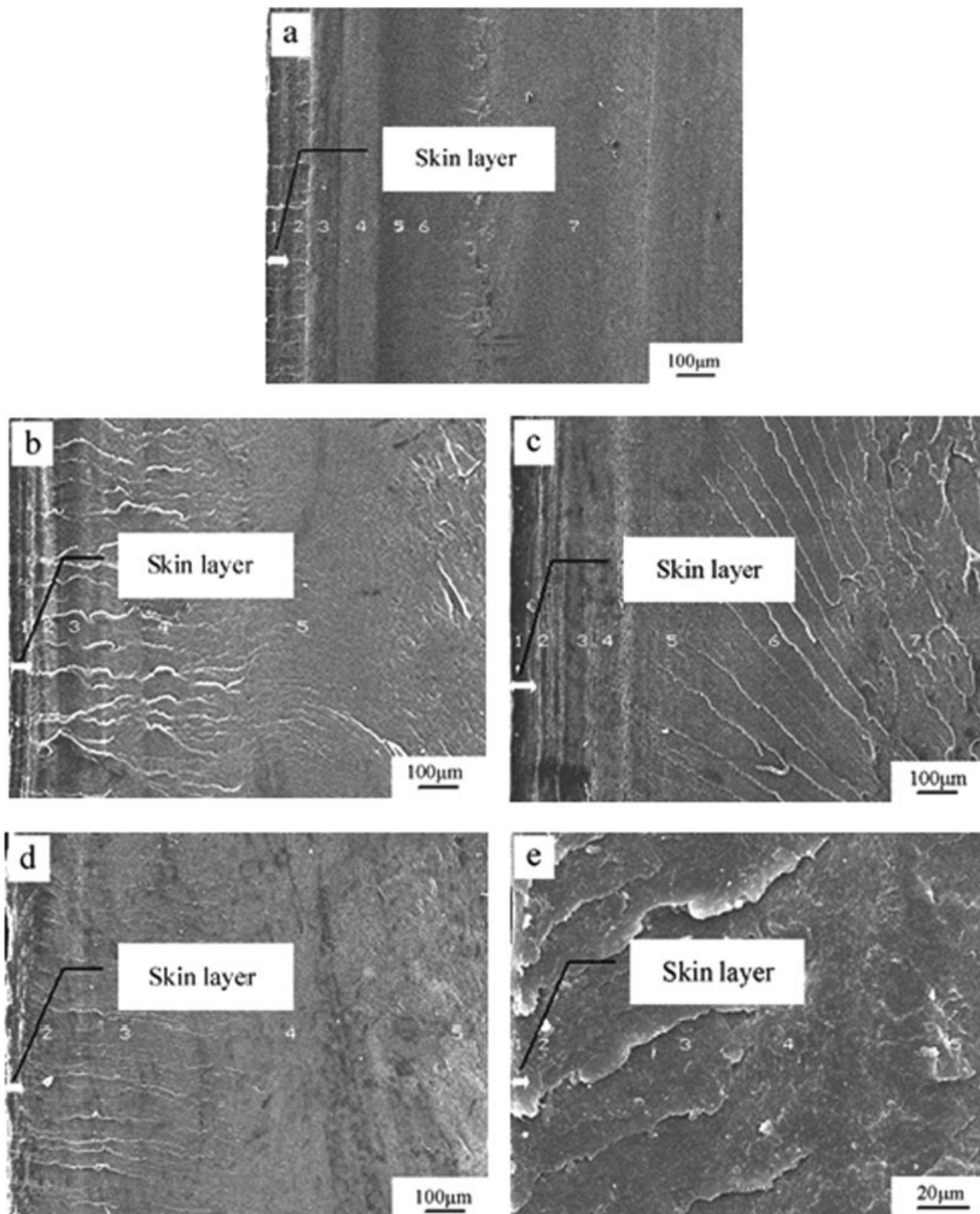


Figure 7 SEM micrographs of samples via different processing conditions in low magnification. (a) sample No. 1, (b) sample No. 3, (c) sample No. 4, (d) sample No. 6, and (e) sample No. 8.

PP.²⁵ Thus, the PP/POE blend in our experiments could be classified as the one with upper critical solution point. According to the SEM photos shown in

Figure 3, the effect of shear stress on the phase morphology is obvious. It is found that the size of the dispersed phase in sample No. 6 is much smaller than

that of sample No. 4, in which the morphology in core layer is cocontinuous. This can also be understood as the result of shear-induced phase mixing. On the other hand, the dispersed phase of sample obtained via lower injection speed is big and highly elongated. As we know, the size and the deformation of a purely viscous (Newtonian) droplet surrounded by another Newtonian fluid is mainly determined by the parameter κ . The parameter κ can be expressed by eq. (1), where σ is the interfacial tension, $\dot{\gamma}$ is the shear rate, and the R is the droplet radius. The physical meaning of the κ term is a balance between the resistance to deformation of the droplet (σ/R) and the local acting shear stress ($\eta_M \dot{\gamma}$) which deforms the droplet. According to this, the smaller the droplets, the greater the resistance to the deformation, and the larger droplets in immiscible systems will be deformed more than those in the miscible blends during the flow field.

$$\kappa = \frac{\sigma}{\eta_M \dot{\gamma} R} \quad (1)$$

CONCLUSIONS

The phase morphology and mechanical properties of the injection-molded samples prepared via different processing conditions have been investigated in detail. A skin-core structure was found and the phase morphology developed gradually from subskin to core layer. Higher barrel temperature, lower mold temperature and higher injection speed resulted in a smaller size of dispersed POE phase. The tensile strength and impact strength were found to be not sensitive to barrel temperature and mold temperature, but also to the low injection speed, both tensile strength, and impact strength had a higher value for specimen obtained via low injection speed. The formation of the skin-core morphology and the effect of

processing conditions on the phase morphology could be understood based on crystallization kinetic of PP matrix, rheology, and shear induced phase mixing.

References

1. Porfyrakis, K.; Assender, H. E.; Robinson, I. M. *Polymer* 2002, 43, 4769.
2. Chiu, C. P.; Hsieh, M. C. *J Eng Mater Tech Trans ASME* 1987, 109, 171.
3. Li, Y.; Ke, W.; Gao, X.; Yuan, Y.; Shen, K. *J Macromol Sci Phys* 2005, 44, 289.
4. Weing, W.; Herzog, F. *J Appl Polym Sci* 1993, 50, 2163.
5. Phillips, R.; Herbert, G.; News, J.; Wolkwicz, M. *Polym Eng Sci* 1994, 34, 1731.
6. Kalay, G.; Bevis, M. J. *J Polym Sci Part B: Polym Chem* 1997, 35, 265.
7. Zhang, X. M.; Aji, A. *Polymer* 2005, 46, 3385.
8. Mendoza, R.; Regnier, G.; Seiler, W.; Lerbun, J. L. *Polymer* 2003, 44, 3363.
9. Martuscelli, E.; Silvestre, C.; Abate, G. *Polymer* 1982, 23, 229.
10. Karger-Kocsis, J.; Csikai, I. *Polym Eng Sci* 1987, 27, 241.
11. Fellahi, S.; Favis, B. D.; Fisa, B. *Polymer* 1996, 37, 2615.
12. Son, Y.; Ahn, K. H.; Char, K. *Polym Eng Sci* 2000, 40, 1376.
13. Fujiyama, M.; Wakino, T.; Kawasaki, Y. *J Appl Polym Sci* 1988, 35, 29.
14. Akay, M.; Ozden, S. *Int Polym Proc* 1996, 11, 179.
15. Madbouly, S. A.; Wolf, B. A. *Macromol Chem Phys* 2003, 204, 417.
16. Wang, Y.; Fu, Q.; Zhang, G.; Shen, K. *Z. Chin J Polym Sci (Engl Ed)* 2003, 21, 505.
17. Yang, J. H.; Zhang, Y.; Zhang, J. X. *Polymer* 2003, 44, 5047.
18. Poon, B. C.; Chum, S. P.; Heltner, A.; Baer, E. *J Appl Polym Sci* 2004, 92, 109.
19. Bedia, E. L.; Murakami, S.; Senoo, K.; Kohjiya, S. *Polymer* 2002, 43, 749.
20. Martuscelli, E. *Polym Eng Sci* 1984, 24, 122.
21. Gauthier, F.; Goldsmith, H. L.; Mason, S. G. *Soc Rheol* 1971, 15, 297.
22. Jefri, M. A.; Zahed, A. H. *Poder Technol* 1984, 37, 255.
23. Wang, Y.; Na, B.; Fu, Q.; Men, Y. F. *Polymer* 2004, 45, 207.
24. Hindawi, I. A.; Higginst, J. S.; Weiss, R. A. *Macromolecules* 1990, 23, 670.
25. McNally, T.; Mcshane, P.; Nally, G. M.; Murphy, W. R.; Cook, M.; Miller, A. *Polymer* 2002, 43, 3785.